

## Physical and Chemical Properties of Cement Mortar with Gamma-C<sub>2</sub>S

Sung-Hyun Lee, Kyungnam Kim, Mabudo<sup>‡</sup>, and Myong-Shin Song<sup>\*†</sup>

*Department of Advanced Materials Engineering, Kangwon National University, Samcheok 25913, Korea*

*\*Research Center of Advanced Convergence Processing on Materials, Kangwon National University, Samcheok 25913, Korea*

(Received August 5, 2015; Revised October 12, 2015; February 25, 2016; Accepted February 26, 2016)

### ABSTRACT

Presently, for the cement industry, studies that seek to reduce CO<sub>2</sub>, because of the development of the plastic industry and demand for reduction of energy use, have been actively conducted among them, studies attempting to use Gamma-C<sub>2</sub>S( $\gamma$ -C<sub>2</sub>S) to fix CO<sub>2</sub> have been actively conducted. The  $\gamma$ -C<sub>2</sub>S compound has an important function in reacting to CO<sub>2</sub> and stiffening through carbonatization in the air. The  $\gamma$ -C<sub>2</sub>S compound, reacting to CO<sub>2</sub> in the air, generates CaCO<sub>3</sub> within the pore structure of cement materials and densifies the pore structure this leads to an improvement of the durability and to the characteristic of resistance against neutralization. Therefore, in this experiment, in order to synthesize  $\gamma$ -C<sub>2</sub>S, limestone sludge and waste foundry sands are used these materials are plasticized for 30 or 60 minutes at 1450°C, and are prevented from being cooled in the temperature range of 30 ~ 1000°C when they are about to be cooled. XRD analysis and XRF analysis are used to determine the effects of this process on  $\gamma$ -C<sub>2</sub>S synthesization, the temperature at which a thing is plasticized, and the conditions for cooling that obtain in the plasticized clinker also, in order to confirm the CO<sub>2</sub> capture function, analysis of the major hydration products is conducted through an analysis of carbonatization depth and compressive strength, and through MIP analysis and XRD Rietveld analysis. As a result of these analyses, it is found that when  $\gamma$ -C<sub>2</sub>S was synthesized, the clinker that was plasticized at 1450°C for one hour demonstrated the highest yield rate the sample with which the  $\gamma$ -C<sub>2</sub>S was mixed generated CaCO<sub>3</sub> when it reacted with CO<sub>2</sub> therefore, carbonatization depth and porosity were reduced, and the compressive strength was increased.

**Key words :** CO<sub>2</sub> capture, Pore, Vaterite, Gamma-C<sub>2</sub>S

### 1. Introduction

Recently, environmental issue, CO<sub>2</sub> emission trading system has been emerged globally. Cement industry, among various sectors, is the field that has consumed more resources and energy, resulting in CO<sub>2</sub> emissions totaling 70 million tons annually. Concrete that has long been used in civil and building work comprises mostly cement which is mixed with aggregate, water and admixture and consumption has still been on the rise thanks to such advantages as low price and high strength. Consequently, consumption of cement has been increasingly growing causing CO<sub>2</sub> emissions to rise accordingly and such increase also has caused environmental problem. Thus cement industry has made efforts to reduce CO<sub>2</sub> emissions and one of typical measures taken is adding industrial byproducts including fly ash and furnace slag to cement as admixture and another is CO<sub>2</sub> capture and storage using the characteristics of the mate-

rial. The method of replacing and adding industrial byproducts to cement is the most common way, which however has the problem in achieving early compressive strength comparing to cement. On the other hand, the material for CO<sub>2</sub> capturing and storing is gamma-C<sub>2</sub>S( $\gamma$ -C<sub>2</sub>S) which is air hardening material which is not responsive to water, but to CO<sub>2</sub>.<sup>1)</sup> Based on such  $\gamma$ -C<sub>2</sub>S compositing technology, the study on composition using CaCO<sub>3</sub> and sand has been underway and application to the field was attempted in Japan. In this study, waste foundry sand that replaces the natural sand was used as SiO<sub>2</sub> source for the purpose of CO<sub>2</sub> capture and limestone (Yonghyun, Dogye) was used as CaCO<sub>3</sub> source so as to develop and test the way of composing  $\gamma$ -C<sub>2</sub>S using waste resource. And fly ash that contains high content of CaO was used as CaO source, thereby reducing CO<sub>2</sub> emissions generated by pyrolysis of limestone. To identify the optimal composition condition for  $\gamma$ -C<sub>2</sub>S using waste foundry sand, limestone and fly ash, burning condition and cooling condition were reviewed and the effect on  $\gamma$ -C<sub>2</sub>S composition yield depending on substitution by fly ash was checked and  $\gamma$ -C<sub>2</sub>S composed was mixed with cement paste to check the performance of CO<sub>2</sub> capture so as to monitor the basic properties and the change to the properties through reaction with CO<sub>2</sub>.

---

<sup>†</sup>Corresponding author : Myong-Shin Song  
E-mail : msong0422@kangwon.ac.kr  
Tel : +82-33-570-6558 Fax : +82-33-570-6558

<sup>‡</sup>Corresponding author : Mabudo  
E-mail : gmabudo@gmail.com  
Tel : +82-33-570-6560 Fax : +82-33-570-6560

## 2. Experimental Procedure

### 2.1. Experiment material

The material used in this experiment was Type I Portland cement (DongYang. Co.Ltd) and the components were as Table 1. Limestone which is the raw material to compose  $\gamma$ -C<sub>2</sub>S was taken from Dogye (D-CaCO<sub>3</sub>) and Yonghyun (Y-CaCO<sub>3</sub>), Gangwon Province and in addition, fly ash which is the byproduct from fluidized-bed boiler and waste foundry sand (WFS) were used and chemical composition of the materials according to XRF analysis is as Table 2. As a result of x-ray diffraction analysis (XRD, Rigaku Ultima II diffractometer, Japan), it's found to have comprised of CaO and CaSO<sub>4</sub> (Fig. 1) and using fly ash, Y-CaCO<sub>3</sub>, D-CaCO<sub>3</sub> and WFS,  $\gamma$ -C<sub>2</sub>S was composed and each material was dried at 105°C for 24 h and crushed for use.<sup>2)</sup>

### 2.2 Calcination process

Based on molar ratio of two types of limestone which is CaO source and WFS which is SiO<sub>2</sub> source, limestone and WFS were mixed at 5:1 though it's 2:1 for reagent before pouring into the mould and was produced in pellet form by 20 MPa hand-pressing. According to calcination condition, it was left at 900°C for 30 minutes while increasing the temperature at the rate 10°C/min which was then increased again to 1,450°C at the rate of 10°C/min and maintained for 30 minutes. The the sample underwent furnace cooling to 200°C before taking out from the furnace and cooling at room temperature. Dusting by volume expansion occurred with the sample which was taken out from electric furnace (Fig. 2) and after cooling completely, the sample was crushed by ball mill.<sup>3)</sup>

### 2.3 Preparation of sample and experiment method

XRD analysis was conducted to identify the components of  $\gamma$ -C<sub>2</sub>S quantitatively. Measurement was carried out at 4°/min in the range of 2 theta 0 ~ 80°. Then XRD-Rietveld analysis was conducted for quantitative analysis and for CO<sub>2</sub> capture test using  $\gamma$ -C<sub>2</sub>S, mortar sample was produced according to KS L 5105, which underwent water curing at 20°C for 24 h and accelerated curing at RH 65% 40°C for 3

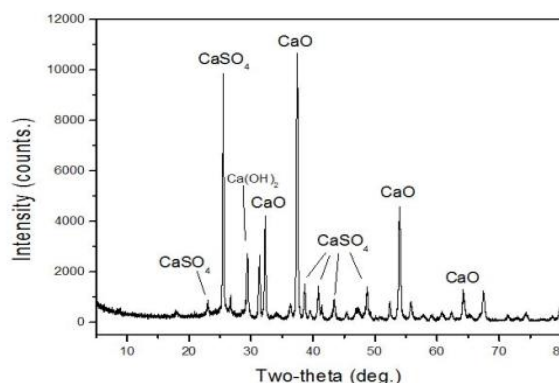


Fig. 1. X-ray diffraction patterns of fly ash.



Fig. 2. Dusting responses during cooling after sintering: (a) Before Sintering, (b) After Sintering

days. The sample after curing process underwent curing process in carbonatization chamber at CO<sub>2</sub> 10%, 20°C, RH 60% for 28 days. Carbonatization depth of the sample was measured by Phenolphthalein method (KS F 2596) Compressive strength test of the samples after carbonatization process was conducted using Universal Testing Machine (UTM) so as to check the effect of  $\gamma$ -C<sub>2</sub>S on carbonatization. And to identify the effect of cement hydrate mixed with  $\gamma$ -C<sub>2</sub>S in carbonatization process, cement paste by substituting  $\gamma$ -C<sub>2</sub>S at 5% and 10%, respectively was produced. Cement paste sample was submerged into acetone for 24 h and dried at 50°C and crushed by ball mill. The grain size after such process was 106  $\mu$ m or less and the sample in the form of fine particle was measured by XRD analysis while the porosity of the sample in the form of 2mm bulk was measured (MIP, Micromeritics, Auto pore IV 9520).<sup>4)</sup>

Table 1. Physical Properties and Chemical Composition of OPC

SiO <sub>2</sub> %	Al <sub>2</sub> O <sub>3</sub> %	CaO%	MgO%	Fe <sub>2</sub> O <sub>3</sub> %	Na <sub>2</sub> O%	K <sub>2</sub> O%	SO <sub>3</sub> %	Specific gravity	Blaine (cm <sup>2</sup> /g)
17.30	4.08	66.50	3.02	3.13	0.09	1.33	3.25	3.15	3,412

Table 2. Chemical Composition as Determined by XRF (wt.%)

	CaO	CO <sub>2</sub>	SiO <sub>2</sub>	Al <sub>2</sub> O <sub>3</sub>	MgO	K <sub>2</sub> O	Fe <sub>2</sub> O <sub>3</sub>	SO <sub>3</sub>	Others	Total
Y-CaCO <sub>3</sub> <sup>a)</sup>	51.80	41.10	3.28	2.09	0.50	0.48	0.40	0.0285	0.32	100
D-CaCO <sub>3</sub> <sup>b)</sup>	51.80	43.60	0.68	0.34	2.98	0.09	0.37	0.0366	0.10	100
WFS <sup>c)</sup>	0.13	-	97.00	1.83	0.05	0.34	-	-	0.65	100
Fly ash	65.61	-	1.15	0.56	2.57	-	0.62	21.48	7.85	-

<sup>a)</sup>CaCO<sub>3</sub> - Yonghyun in Korea

<sup>b)</sup>CaCO<sub>3</sub> - Dogea in Korea

<sup>c)</sup>Waste foundry sand

### 3. Results and Discussion

#### 3.1 $\gamma$ -C<sub>2</sub>S composition yield depending on type of CaCO<sub>3</sub>

C<sub>2</sub>S  $\gamma$  polymorph is generated during the process when  $\beta$  (bet) is converted to  $\gamma$  (gamma) In tetrahedral rotation of SiO<sub>4</sub> and atomic calcium migration, particles are split into smaller particles while the volume is increased by 12% which is called dusting.<sup>9)</sup> Fig. 3 shows diffraction pattern according to XRD analysis of the sample calcinated by mixing D-CaCO<sub>3</sub>, Y-CaCO<sub>3</sub>, WFS powder. As a result of XRD analysis, with regard to  $\gamma$ -C<sub>2</sub>S peak appeared around 2theta 29.5°, peak intensity of the sample using Y-CaCO<sub>3</sub> was higher than the sample using D-CaCO<sub>3</sub>. As a result of XRD-Rietveld analysis, the sample using Y-CaCO<sub>3</sub> contained 94.4 wt.% while the sample using D-CaCO<sub>3</sub> contained 46.7 wt.% of  $\gamma$ -C<sub>2</sub>S, which indicated that the difference in composition by origin had a significant effect on generation of  $\gamma$ -C<sub>2</sub>S, which was attributable to difference in composition yield due to Mg ion used as stabilizer or impurities during composing  $\gamma$ -C<sub>2</sub>S when changing from  $\beta$  to  $\gamma$ . Thus, Y-CaCO<sub>3</sub> which generates more  $\gamma$ -C<sub>2</sub>S in sample after calcination process was applied to CO<sub>2</sub> capture test.

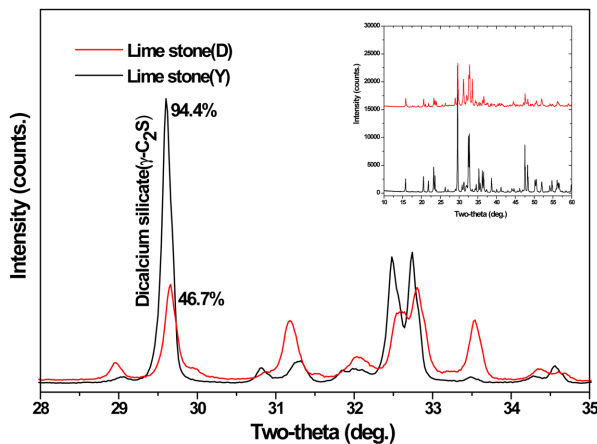


Fig. 3. XRD analysis results of synthesized  $\gamma$ -C<sub>2</sub>S.

#### 3.2 Variation of $\gamma$ -C<sub>2</sub>S composition depending on cooling condition

In composition of  $\gamma$ -C<sub>2</sub>S using waste resources, the effect of cooling condition after calcination process on  $\gamma$ -C<sub>2</sub>S dusting and generation was reviewed. After firing the clinker at 1,450°C for 30 minutes and setting the discharge temperature of electric furnace at 1000, 800, 600, 400, 200 and 30°C, the samples were cooled down at room temperature. Then  $\gamma$ -C<sub>2</sub>S peak was checked using XRD analysis. Fig. 4 shows the difference in XRD peak intensity depending on discharge temperature for cooling in composition of  $\gamma$ -C<sub>2</sub>S. There's a slight difference in peak of samples after burning at set temperature and discharged at different conditions but the effect of discharge temperature on generation of  $\gamma$ -C<sub>2</sub>S was considered insignificant. That is, difference in discharge temperature after burning at set temperature was not influential on phase inversion from  $\beta$ -C<sub>2</sub>S to  $\gamma$ -C<sub>2</sub>S

#### 3.3 Effect of ash fly on composition of $\gamma$ -C<sub>2</sub>S

Table 3 shows generation of  $\gamma$ -C<sub>2</sub>S when replacement rate of fly ash to the limestone to be abandoned after cement manufacture is 0, 0.5, 1.0, 3.0 and 5.0 wt.%, which resulted from XRD-Rietveld analysis of the sample produced using Y-CaCO<sub>3</sub> and waste foundry sand (WFS) Replacement rate

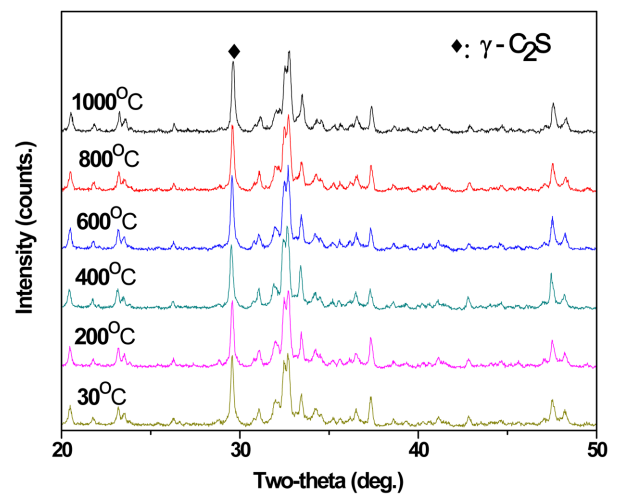


Fig. 4 XRD analysis results of cooling temperatures.

Table 3.  $\gamma$ -C<sub>2</sub>S Yield Variation in Fly Ash Replacement Ratio over the XRD- Rietveld Analysis

Profile ID	Fly ash replacement ratio by weight of CaCO <sub>3</sub>					
	0 wt.%	0.5 wt.%	1.0 wt.%	3.0 wt.%	5.0 wt.%	
Dicalcium silicate - Ca <sub>2</sub> (SiO <sub>4</sub> )	91.4	78.3	74.6	60.6	37.5	
Calcium silicate - Ca <sub>2</sub> SiO <sub>4</sub>	-	0.3	1.2	1.6	1.3	
Calcium silicate - Ca(SiO <sub>3</sub> )	-	-	-	-	-	
Lime - CaO	-	11.4	9.3	11.9	16.0	
Larnite - Ca <sub>2</sub> SiO <sub>4</sub>	-	-	7.7	19.0	38.6	
Akermanite - Ca <sub>2</sub> Mg(Si <sub>2</sub> O <sub>7</sub> )	8.6	-	-	-	-	
Hatruite - Ca <sub>3</sub> SiO <sub>5</sub>	-	10.0	7.2	6.9	6.6	
Total	100.0	100.0	100.0	100.0	100.0	

of fly ash was appeared to have had a significant effect on generation of  $\gamma$ -C<sub>2</sub>S. When replacement rate of fly ash is increased, generation of  $\gamma$ -C<sub>2</sub>S tends to reduce (Fig. 5) which is attributable to impurities or ion used as stabilizer as shown in the result depending on origin of limestone.<sup>6)</sup> It's reported by previous studies that inversion from  $\beta$ -C<sub>2</sub>S to  $\gamma$ -C<sub>2</sub>S is constrained by adding proper impurities such as boron. Further study on such impurities is necessary to identify the cause of such phenomenon.

### 3.4 CO<sub>2</sub> capture of composed $\gamma$ -C<sub>2</sub>S

Composed  $\gamma$ -C<sub>2</sub>S was mixed with 7.5 wt.% water and the sample with the density 1,550 kg/m<sup>3</sup> was produced through the process of isostatic pressing into a small cylindrical shape and the sample underwent accelerated carbonatization process by exposing to high purity CO<sub>2</sub> for 28 and 56 days, respectively. Fig. 6 shows the result of XRD analysis intended to check CO<sub>2</sub> capture effect of  $\gamma$ -C<sub>2</sub>S in each sample. C<sub>2</sub>S and Ca(OH)<sub>2</sub> hydrate were detected from the sample which was not exposed to low CO<sub>2</sub> but Ca(OH) peak during CO<sub>2</sub> curing was dissipated after reaction with CO<sub>2</sub> and vaterite CaCO<sub>3</sub> hydrate including calcite CaCO<sub>3</sub> was found which was attributable to vaterite CaCO<sub>3</sub> as a result of reaction of Ca(OH)<sub>2</sub> with CO<sub>2</sub> and the reaction between  $\gamma$ -C<sub>2</sub>S and unreacted CaO and CO<sub>2</sub>. Thus it's expected that  $\gamma$ -C<sub>2</sub>S will collect CO<sub>2</sub> thereby reducing CO<sub>2</sub> in the air and when applying mortar, CaCO<sub>3</sub> product will reduce the porosity and increase the compressive strength.

### 3.5. Characteristics of compressive strength

Figure 7 shows the compressive strength of cement mortar sample containing  $\gamma$ -C<sub>2</sub>S at replacement rate 5 and 10 wt.% and ordinary cement mortar without  $\gamma$ -C<sub>2</sub>S. Comparison between mortar sample without carbonatization process and the sample after carbonatization process with 10% CO<sub>2</sub> for 28 days and 56 days was made. When replacing  $\gamma$ -C<sub>2</sub>S by 10% or more, hardened cement paste becomes collapsed because of excessive reactivity due to unreactive CaO in  $\gamma$ -C<sub>2</sub>S. Viewing the result, the more the replacement rate the less the cement weight and the less the compressive strength before carbonatization process, but in case of the

sample containing carbonized  $\gamma$ -C<sub>2</sub>S ( $\gamma$ -C<sub>2</sub>S replacement rate 5, 10 wt.%), compressive strength was increased than OPC ( $\gamma$ -C<sub>2</sub>S replacement rate 0 wt.%) which was attributable to forming CaCO<sub>3</sub> crystal phase by  $\gamma$ -C<sub>2</sub>S through reaction with CO<sub>2</sub> in hardened cement paste that increased the compressive strength by reducing the porus in cement.

### 3.6 Porosity of hardened cement paste mixed with synthetic $\gamma$ -C<sub>2</sub>S

Figure 8 shows the porosity of mortar sample produced using  $\gamma$ -C<sub>2</sub>S which has superior performance in compressive strength and penetration depth in a way of replacing  $\gamma$ -C<sub>2</sub>S 10 wt.% before and after carbonatization. A rapid decrease in porosity appeared in porus less than 100  $\mu$ m because of CaCO<sub>3</sub> generated by reaction between  $\gamma$ -C<sub>2</sub>S and CO<sub>2</sub> at carbonatization condition, comparing to standard condition. Such result is attributable to CaCO<sub>3</sub> generated in porus in hardened cement paste. Porosity was 29.0% at standard curing condition which was reduced to 19.4% when curing

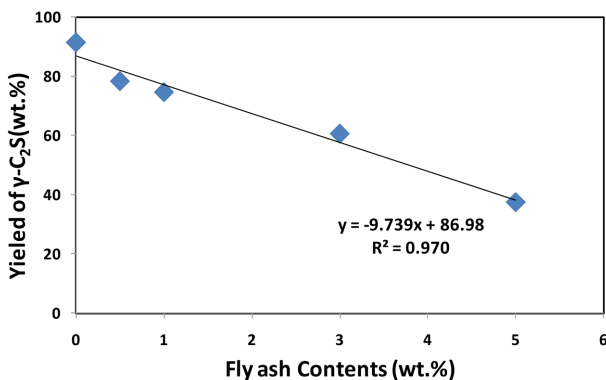


Fig. 5. Yield of  $\gamma$ -C<sub>2</sub>S by fly ash replacement ratio.

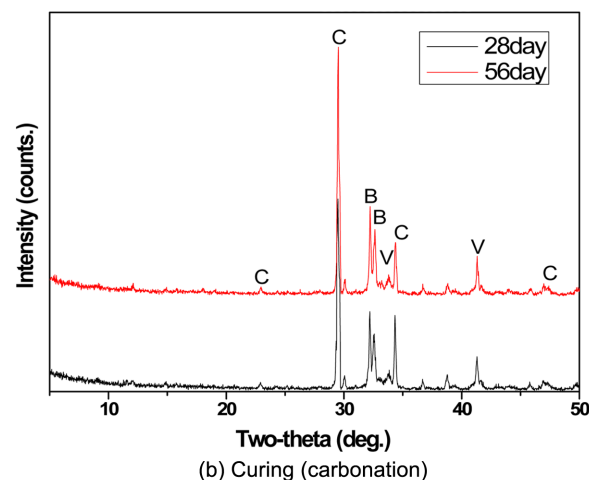
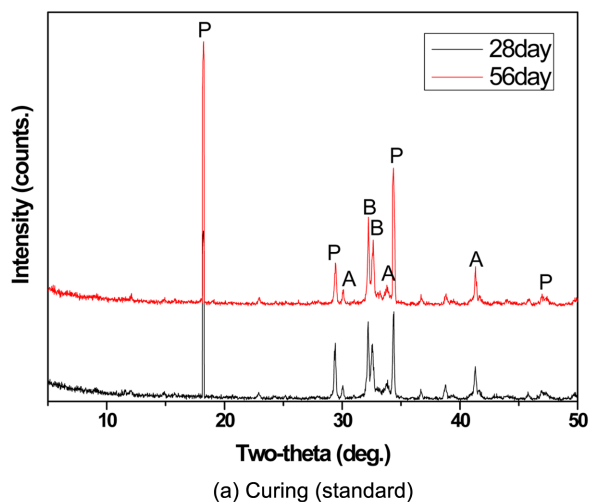


Fig. 6. XRD results of each paste after CO<sub>2</sub> reaction. (a) P : Portlandite(Ca(OH)<sub>2</sub>), A : Alite(C<sub>3</sub>S), B : Belite(C<sub>2</sub>S), (b) C : Calcite(CaCO<sub>3</sub>), V :Vaterite(CaCO<sub>3</sub>), B : Belite (C<sub>2</sub>S)

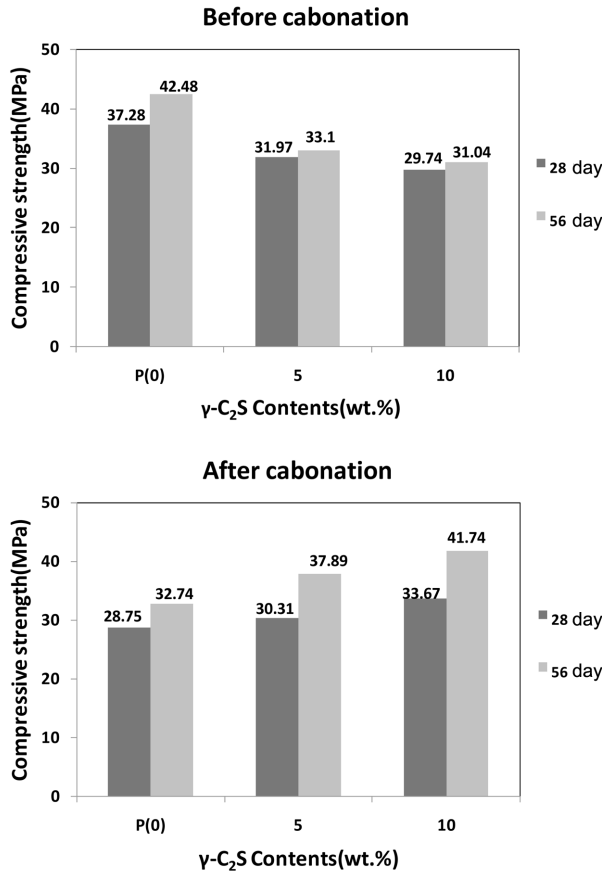


Fig. 7. Changes of compressive strength of mortar.

the same sample at carbonatization condition (Table 4) Such reduction resulted from calcite(CaCO<sub>3</sub>) and vaterite(CaCO<sub>3</sub>) generated as a result of reaction between  $\gamma$ -C<sub>2</sub>S and CO<sub>2</sub> by carbonatization that resulted in densifying the structure.

### 3.7 Mixing $\gamma$ -C<sub>2</sub>S with hardened cement paste and CO<sub>2</sub> capture

To identify CaCO<sub>3</sub> generated after curing cement mortar by replacing  $\gamma$ -C<sub>2</sub>S 10% in carbonatization chamber set as CO<sub>2</sub> density 10%, temperature 20°C and humidity 60% for 56 days, XRD-riedveld analysis was conducted. Viewing the analysis result in Table 5, OPC in case of 19.58%,  $\gamma$ -C<sub>2</sub>S replacing, 31.24% of CaCO<sub>3</sub> was generated. Consequently,

Table 4. Porosity Change of Paste Containing  $\gamma$ -C<sub>2</sub>S

type	Standard curing	Carbonation curing	Porosity reduction(%)
Porosity(%)	29.0	19.4	33.1

Table 5. CO<sub>2</sub> Capture Rate through Carbonation

type	CaCO <sub>3</sub> amount		CO <sub>2</sub> capture (%)
	OPC	$\gamma$ -C <sub>2</sub> S (10%)	
Carbonation	19.58%	31.24%	59.5%

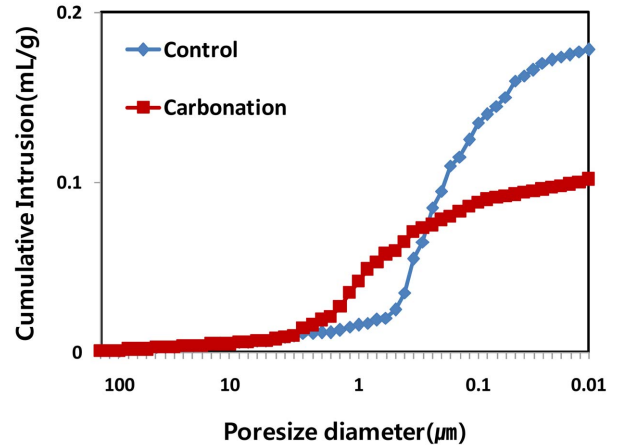


Fig. 8. Porosity analysis of the paste.

CaCO<sub>3</sub> generation by CO<sub>2</sub> capture was more than OPC by 11% and in case of replacing  $\gamma$ -C<sub>2</sub>S 10%, 59.5% CO<sub>2</sub> capture was achieved. .

CO<sub>2</sub> emission per ton of cement in Korea is 0.856 ton and when composing  $\gamma$ -C<sub>2</sub>S, it's 0.274ton. Thus, in case of replacing  $\gamma$ -C<sub>2</sub>S 10%, CO<sub>2</sub> emission would be 0.798 ton which is less than cement and 0.475 ton would be captured by CO<sub>2</sub> capture.

## 4. Conclusions

1. As a result of accelerated carbonatization of  $\gamma$ -C<sub>2</sub>S for 28 & 56 days, vaterite and calcite were formed.
2. According to measuring carbonatization penetration depth, the more replacement of  $\gamma$ -C<sub>2</sub>S the less porous and penetration depth because of generation of vaterite and calcite.
3. After carbonatization of mortar by replacing 10 wt.% to OPC, compressive strength of mortar mixed with  $\gamma$ -C<sub>2</sub>S with replacement rate 10 wt.% was higher than OPC because of CaCO<sub>3</sub> generated as a result of reaction between  $\gamma$ -C<sub>2</sub>S and CO<sub>2</sub> that resulted in densifying the porous.
4. As a result of measuring the porosity of hardened cement paste, porosity of cement paste after replacing  $\gamma$ -C<sub>2</sub>S 10 wt.% was less than cement paste without using  $\gamma$ -C<sub>2</sub>S by 33.1% which indicated mixing  $\gamma$ -C<sub>2</sub>S with hardened cement paste would increase CO<sub>2</sub> capture as well as compressive strength and CO<sub>2</sub> capture rate was 59.5% which is able to achieve the capture of 0.475 ton CO<sub>2</sub> in case of replacing  $\gamma$ -C<sub>2</sub>S 10%.

Thus, when replacing and adding  $\gamma$ -C<sub>2</sub>S to cement material, CaCO<sub>3</sub> in various phases is generated by reaction between  $\gamma$ -C<sub>2</sub>S and CO<sub>2</sub> in the air at early stage which densifies the porous in cement. It creates the effect to enhance the compressive strength more than cement material without  $\gamma$ -C<sub>2</sub>S. In cement material exposed to the air containing CO<sub>2</sub>, CO<sub>2</sub> is the major cause to neutralize the cement material. But cement material containing  $\gamma$ -C<sub>2</sub>S densifies the

poris in cement at early stage so as to retard penetration or expansion of CO<sub>2</sub>. That is, cement material containing  $\gamma$ -C<sub>2</sub>S performs carbonatization response by CO<sub>2</sub> penetrated from outside which results in densifying the porous structure of cement material at early stage and CO<sub>2</sub> penetration and expansion are delayed. Obviously, it's necessary to identify the relationship between neutralization resistance and CO<sub>2</sub> penetration and expansion so as to verify the effect of optimal use of  $\gamma$ -C<sub>2</sub>S.

## REFERENCES

1. C.-W. Park, "Eco-Friendly of Concrete," *Mag. Korea Concr. Inst.*, **20** [6] 24-6 (2008).
2. S.-H. Lee, "Hydration Mechanism of Ground Granulated Blast Furnace Slag," *Mag. Korea Concr. Inst.*, **24** [6] 31-4 (2012).
3. J. I. Escalante-Garcia, "Portland Cement-Blast Furnace Slag Mortars Activated Using Waterglass: Effect of Temperature and Alkali Concentration," *Construct. Build. Mater.*, **66** 323-28 (2014).
4. K. J. Mun, "The Effect of Slaked Lime, Anhydrous Gypsum and Limestone Powder on Properties of Blast Furnace Slag Cement Mortar and Concrete," *Construct. Build. Mater.*, **21** 1576-82 (2007).
5. H. Sakamoto, "pH Behavior of Hydrated Low-Alkalinity Cement," *J. Nucl. Fuel Cycle Environ.*, **5** [2] 37-42 (1999).
6. F. Winnefeld, "Hydration of Calcium Sulfo-Aluminate Cements - Experimental Findings and Thermodynamic Modelling," *Cem. Concr. Res.*, **40** 1239-47 (2010).